Supplementary Information for

Enhanced transformation of aquatic organic compounds by long-lived photooxidants (LLPO) produced from dissolved organic matter

Stephanie Christa Remke,[†,‡] *Urs von Gunten,*[†,‡] and *Silvio Canonica*[*,†]

[†]Eawag, Swiss Federal Institute of Aquatic Science and Technology, Überlandstrasse 133, CH-8600 Dübendorf, Switzerland

[‡]School of Architecture, Civil and Environmental Engineering (ENAC), Ecole Polytechnique Fédérale de Lausanne (EPFL), GC A2 454, Station 18, CH-1015 Lausanne, Switzerland

*To whom correspondence should be addressed.

E-mail: silvio.canonica@eawag.ch Telephone: +41-58-765-5453

Text S1. Estimation of the lifetime of LLPO

Two deactivation pathways for LLPO are considered.

1) A hypothetical unimolecular decay of LLPO, with first-order rate constant $k_{LLPO}^{d,0}$.

$\quad$ LLPO → LLPO$_{deact}$ $\hspace{8cm}$ (S1)

2) The reaction of LLPO with a target compound (TC).

$\quad$ LLPO + TC → LLPO$_{deact}$ + TC$_{ox}$ $\hspace{5cm}$ (S2)

The pseudo-first-order rate constant attributed to this reaction is the product of the second-order-rate constant $k_{LLPO,TC}$ for the reaction of LLPO with the TC and the concentration of the target compound ($[TC] \approx [TC]_0$), i.e. $k_{LLPO,TC} \times [TC]$. We estimate a maximum $k_{LLPO,TC}$ value of $3 \times 10^9 \text{ M}^{-1}\text{ s}^{-1}$ for electron-rich phenols based on a review of available experimental second-order rate constants for organic peroxyl radicals (Neta et al. 1990) and phenoxyl radicals (Neta and Grodkowski 2005).

The overall deactivation of LLPO in the presence of TC can be described by the pseudo-first-order rate constant k_{LLPO}^d:

$$k_{LLPO}^d = k_{LLPO}^{d,0} + k_{LLPO,TC} [TC] \hspace{4cm} (S3)$$

Assuming an at least 50% reduction of the steady-state concentration of LLPO upon addition of TC at $[TC] = 5 \times 10^{-6}$ M, which corresponds (at an unchanged formation rate of LLPO) to the condition:

$$k_{LLPO,TC} [TC] > k_{LLPO}^{d,0} \hspace{4cm} (S4)$$

and substituting the mentioned numeric values of $k_{LLPO,TC}$ and $[TC]$ into eq. (S4), one obtains $k_{LLPO}^{d,0} < 1.5 \times 10^4 \text{ s}^{-1}$, corresponding to an LLPO lifetime $\tau_{LLPO} = k_{LLPO}^{d\ -1} > 67$ μs.

This lifetime is in a similar range as estimated in a previous study (> 100 μs) (Canonica and Hoigné 1995).

Text S2. Estimation of the lifetime of ^{3}CDOM*

We refer here to the methodology used in a previous review article (Rosario-Ortiz and Canonica 2016) and Scheme 1 in the main paper. Accordingly, the pseudo-first-order deactivation rate constant of ^{3}CDOM* in the presence of a target compound (TC) can be defined as:

$$k^d_{^3CDOM^*} = k^{d,0}_{^3CDOM^*} + k^q_{^3CDOM^*,O_2}[O_2] + k^q_{^3CDOM^*,TC}[TC] \qquad (S5)$$

where $k^{d,0}_{^3CDOM^*}$ is the first-order-deactivation rate constant of ^{3}CDOM*, $k^q_{^3CDOM^*,O_2}$ is the second-order rate constant for the quenching of ^{3}CDOM* by oxygen, $[O_2]$ is the oxygen concentration, $k_{^3CDOM^*,TC}$ is the second-order rate constant for the quenching of ^{3}CDOM* by the target compound, and [TC] is the concentration of the latter. Correspondingly, the lifetime of ^{3}CDOM* is defined as:

$$\tau_{^3CDOM^*} = k^d_{^3CDOM^*}{}^{-1} \qquad (S6)$$

In the case of [TC] < 10 µM, $k_{^3CDOM^*,TC}[TC] \ll k^{d,0}_{^3CDOM^*} + k^q_{^3CDOM^*,O_2}[O_2]$, and eq. (S5) simplifies to:

$$k^d_{^3CDOM^*} = k^{d,0}_{^3CDOM^*} + k^q_{^3CDOM^*,O_2}[O_2] \qquad (S7)$$

For $k^{d,0}_{^3CDOM^*}$ and $k^q_{^3CDOM^*,O_2}$ different values were proposed in the literature. Sharpless et al. (Sharpless 2012) estimated a ^{3}CDOM* lifetime of $\approx$ 20 µs in the absence of oxygen (i.e., $k^{d,0}_{^3CDOM^*} = 5 \times 10^4$ s^{-1}). Schmitt et al. (2017) measured lifetimes between 12 − 26 µs, for different natural water (i.e., $k^{d,0}_{^3CDOM^*} = (3.8 − 8.3) \times 10^4$ s^{-1}). Zepp et al. (1985) proposed $k^q_{^3CDOM^*,O_2} = 2 \times 10^9$ M^{-1} s^{-1}, based on quenching rate constants of organic photosensitizers. In aerated waters ([O$_2$] = 258 µM) this leads to lifetimes of around 2 µs ($k^q_{^3CDOM^*,O_2}[O_2] = 5 \times 10^5$ s^{-1}). Golanoski et al. (2012) determined values of $k^q_{^3CDOM^*,O_2}$ in the range of 0.5 − 2.1 $\times 10^9$ M^{-1} s^{-1}. Taking all the above different measurements of $k^{d,0}_{^3CDOM^*}$ and $k^q_{^3CDOM^*,O_2}$ into consideration, the lifetimes of ^{3}CDOM* in aerated water at 25 °C and normal atmospheric pressure are expected to fall in the range of 1.6 − 6.3 µs.

Table S1. HPLC methods for the analysis of individual compounds [a]

Compound	Eluent composition (%)			Retention time (min)	Absorption wavelength / nm (Photodiode array detector)	Excitation/Emission wavelength / nm (Fluorescence detector)
	water	acetonitrile	buffer [b]			
phenol	-	30	70	3.3	220	275/310
4-methylphenol	-	40	60	3.2	220	225/316
2,4,6-trimethylphenol	-	20	80	4.1	220	230/325
3,4-dimethoxyphenol	-	25 [c]	75 [c]	2.7 [c]	220	230/325
trolox	-	43	57	3.3	220	-
DMABN	40	60	-	2.5	298	290/488
4-cyanoaniline	70	30	-	3.0	273	274/384
4-acetylaniline	75	25	-	2.7	312	230/390
aniline	70	30	-	3.0	242	232/343
4-methylaniline	40	60	-	3.0	242	232/343
sulfadiazine	-	15	85	2.7	266	-
sulfamethoxazole	-	15	85	2.6	270	-
sulfadimethoxine	-	20	80	2.2	270	-
isoproturon	55	45	-	2.5	242	-
diuron	-	55	45	2.6	242	-
DMP	55	45	-	2.4	242	-
2-acetonaphthone	-	gradient method [d]		9.5	242	-
4-cyanophenol	-	gradient method [d]		6.5	242	-

[a] All compounds were analyzed on a reverse-phase C_{18} column (COSMOSIL 5C18-MS-II packed column, pore size 120 Å, particle size 5 µm, internal diameter 3.0 mm, length 100 mm) with a column oven temperature of 25 °C (Agilent system) or 30 °C (Dionex system), a flow rate of 0.5 mL min^{-1}, and an injection volume of 100 µL. The employed measuring ranges for phenols, anilines and 2-acetonaphthone were 0.5 – 5 µM with the photodiode array detector, and 0.01 – 0.1 µM with the fluorescence detector, the measuring range for trolox, phenylureas and sulfonamides was 0.01 – 5.0 µM with the photodiode array detector. Standard deviations of measured concentrations were typically < 5 %. [b] Buffer composition: 10 mM H_3PO_4 in ultrapure water, pH=2.1. [c] In the presence of 2-acetonaphthone and 4-cyanophenol, the method described in note d was used, and the retention time was 4.1 min. [d] Time course of the gradient method (acetonitrile (ACN)/buffer): 0.0 min (start), 15% ACN; 3.0 min, 15% ACN; 7.0 min, 70% ACN; 10.8 min, 70% ACN; 12.8 min, 15% ACN; 14 min (stop), 15% ACN.

Text S3. Light screening corrections

Light screening corrections were performed according to the methods developed in previous studies (Leresche et al. 2016, Wenk et al. 2011). In brief, the wavelength-dependent light screening factor of a DOM solution, $S_{\lambda,DOM}([DOM])$, can be calculated based on the following Morowitz-type equation (Morowitz 1950):

$$S_{\lambda,DOM}([DOM]) = \frac{1-e^{-2.303(\varepsilon_{\lambda,DOM}[DOM])b}}{2.303(\varepsilon_{\lambda,DOM}[DOM])b} \tag{S8}$$

where λ (nm) is the wavelength of light, b (cm) is the path length of light through the sample, $\varepsilon_{\lambda,DOM}$ (L mg$_C^{-1}$ cm^{-1}) is the decadic specific absorption coefficient of DOM, and [DOM] is the concentration of DOM (mg$_C$ L^{-1}).

The geometries of the lamp and the sample quartz tubes were taken into consideration to calculate the average optical path length, $\bar{b}$, which was determined to be 1.785 cm, corresponding to the internal diameter of the quartz tubes (1.5 cm) multiplied by a factor of 1.19 (Leresche et al. 2016). Substituting $\bar{b}$ for b in eq. (S8) yields the light screening factor for the specific irradiation conditions of the used photoreactor, $\bar{S}_{\lambda,DOM}([DOM])$. Since the absorption of light in the photoreactor occurs at only two relevant wavelengths, namely 366 nm (major component) and 334 nm (minor component), a wavelength-averaged screening factor, $\bar{S}_{\bar{\lambda},DOM}([DOM])$, was subsequently calculated employing eq. (S9):

$$\bar{S}_{\bar{\lambda},DOM}([DOM]) = \frac{I_{\lambda=334\,nm}T_{\lambda=334\,nm}\bar{S}_{\lambda=334\,nm}+I_{\lambda=366\,nm}T_{\lambda=366\,nm}\bar{S}_{\lambda=366\,nm}}{I_{\lambda=334\,nm}T_{\lambda=334\,nm}\varepsilon_{\lambda=334\,nm}+I_{\lambda=366\,nm}T_{\lambda=366\,nm}\varepsilon_{\lambda=366\,nm}} \tag{S9}$$

Where I_λ is the photon flux emitted by the lamp ($I_{\lambda=334\,nm} = 17 \times 10^{-3}$ mol quantum hour^{-1}; $I_{\lambda=366\,nm} = 236 \times 10^{-3}$ mol quantum hour^{-1}) (Wenk et al. 2011) and T_λ is the transmission of the NaNO$_3$ filter solution used in the photoreactor ($T_{\lambda=334\,nm} = 0.483$; $T_{\lambda=366\,nm} = 0.816$) (Wenk et al. 2011). $\bar{S}_{\lambda,DOM}([DOM])$ values for $\lambda = 366$ and 334 nm were calculated using the specific absorption coefficients of the employed DOM isolates, which were determined at the relevant wavelengths of 366 nm and 334 nm (Table S3) in phosphate-buffered aqueous solutions (5 mM, pH 8.0) with [DOM] in the range of 1 – 10 mg$_C$ L^{-1}.

Light screening corrections of rate constants obtained using DOM solutions were performed by dividing the observed rate constant by the applicable screening factor, $\bar{S}_{\bar{\lambda},DOM}([DOM])$ (see also Text S4).

Table S2. Decadic specific absorption coefficients of the used DOM isolates

DOM Type	$\varepsilon_{334\ nm,DOM}/$ L mg$_C^{-1}$ cm^{-1}	$\varepsilon_{366\ nm,DOM}/$ L mg$_C^{-1}$ cm^{-1}
SRFA	0.0116	0.0087
SRHA	0.0174	0.0164
PLFA	0.0063	0.0241

Table S3. Screening factors ($\overline{S}_{\overline{\lambda},DOM}([DOM])$) for the various DOM types and concentrations

DOM Type	[DOM]/ mg$_C$ L^{-1}			
	1.0	2.5	5.0	10.0
SRFA	0.98	0.95	0.90	0.82
SRHA	0.97	0.93	0.86	0.75
PLFA	0.99	0.97	0.95	0.90

Text S4. Rate constants and corrections

For each target compound, a set of four pseudo-first-order rate constants from duplicate independent experiments was determined, namely $k_{\text{dir\_0.1}}^{\text{obs}}$ and $k_{\text{dir\_5.0}}^{\text{obs}}$, (blank experiments, DOM-free solutions) and $k_{\text{DOM\_0.1}}^{\text{obs}}$, and $k_{\text{DOM\_5.0}}^{\text{obs}}$ (DOM-containing solutions). The subscripts _0.1 and _5.0 are used to designate the initial concentration of the target compound, namely 0.1 µM and 5.0 µM, respectively. In a first step, $k_{\text{DOM}}^{\text{obs}}$ were corrected for the light screening effect (see Text S3 and Table S3) to give $k_{\text{DOM}}^{\text{obs,sc}}$ according to eq. (S10). In a second step, with some exceptions explained below, $k_{\text{DOM}}^{\text{obs,sc}}$ was further corrected for the often minor non-DOM-induced phototransformation (mainly attributed to direct photolysis) by subtracting $k_{\text{dir}}^{\text{obs}}$ to yield $k_{\text{DOM}}^{\text{obs,c}}$, according to eq. (S11).

$$k_{\text{DOM}}^{\text{obs,sc}} = k_{\text{DOM}}^{\text{obs}}/\bar{S}_{\bar{\lambda},\text{DOM}}([\text{DOM}]) \tag{S10}$$

$$k_{\text{DOM}}^{\text{obs,c}} = k_{\text{DOM}}^{\text{obs,sc}} - k_{\text{dir}}^{\text{obs}} \tag{S11}$$

The second correction was not performed in the cases in which $k_{\text{dir}}^{\text{obs}}$ was dominant, thus excluding the determination of the enhancement factor (*EF*) as defined by eq. 2 of the main paper. The phototransformation of aniline and 4-methylaniline at 5 µM initial concentration in the absence of DOM appeared to be significantly affected by an autocatalytic effect. Therefore, $k_{\text{dir\_5.0}}^{\text{obs}}$ was determined in a limited time range. In the case of aniline, $k_{\text{dir\_5.0}}^{\text{obs}}$ was still high compared to $k_{\text{DOM\_5.0}}^{\text{obs,sc}}$. For this reason, $k_{\text{dir\_5.0}}^{\text{obs,c}}$ was obtained by subtracting $k_{\text{dir\_0.1}}^{\text{obs}}$ from $k_{\text{DOM\_5.0}}^{\text{obs,sc}}$. This correction leads to a possible underestimation of *EF* for aniline.

Table S4. Observed and corrected pseudo-first-order transformation rate constants [a] of target compounds used for Fig. 1 in the main paper

Target compound	$k^{obs}_{dir\_0.1}$ [b]	$k^{obs}_{dir\_5.0}$ [b]	$k^{obs,sc}_{SRFA\_0.1}$ [c]	$k^{obs,sc}_{SRFA\_5.0}$ [c]	$k^{obs,c}_{SRFA\_0.1}$ [d]	$k^{obs,c}_{SRFA\_5.0}$ [d]	EF
phenols							
phenol	0.27 ± 0.08	0.10 ± 0.03	2.27 ± 0.01	2.37 ± 0.04	2.00 ± 0.08	2.27 ± 0.06	0.88 ± 0.06
4-methylphenol	0.3 ± 0.2	0.22 ± 0.02	7 ± 2	8.3 ± 0.1	7 ± 2 [e]	8.1 ± 0.2	0.8 ± 0.2
2,4,6-trimethylphenol	< 1	0.39 ± 0.01	190 ± 40	31.9 ± 0.7	190 ± 40 [e]	31.5 ± 0.7	6 ± 1
3,4-dimethoxyphenol	20 ± 10	< 1	1700 ± 100	150 ± 9	1700 ± 100 [e]	150 ± 9 [e]	11 ± 2
trolox	24 ± 3	16 ± 2	1140 ± 50	87 ± 1	1120 ± 50	72 ± 3	16 ± 1
anilines							
DMABN	6.86 ± 0.08	1.8 ± 0.5	17.83 ± 0.03	19 ± 2	11.0 ± 0.1	17 ± 3	0.6 ± 0.1
4-cyanoaniline	0.551 ± 0.002	0.14 ± 0.04	1.48 ± 0.04	1.9 ± 0.4	0.93 ± 0.04	1.7 ± 0.5	0.5 ± 0.2
4-acetylaniline	5.0 ± 0.2	4.8 ± 0.2	7.51 ± 0.04	4.9 ± 0.1	2.5 ± 0.2	n.d. [f]	n.d.
aniline	0.6 ± 0.2	9 ± 2 [g]	10.7 ± 0.2	4.8 ± 0.3	10.1 ± 0.4	4.2 ± 0.5 [h]	2.4 ± 0.4
4-methylaniline	1.4 ± 0.4	1.36 ± 0.02 [g]	28 ± 1	11.93 ± 0.04	27 ± 2	10.6 ± 0.06	2.6 ± 0.2
phenylureas							
diuron	0.73 ± 0.02	0.48 ± 0.02	1.8 ± 0.4	1.10 ± 0.02	1.1 ± 0.5	0.62 ± 0.04	1.7 ± 0.8
isoproturon	0.7 ± 0.5	0.200 ± 0.004	7.1 ± 0.5	6.2 ± 0.1	6.4 ± 0.9	6.0 ± 0.1	1.1 ± 0.2
DMP	7 ± 2	0.9 ± 0.2	63 ± 1	24.3 ± 0.7	56 ± 3	23.4 ± 0.9	2.4 ± 0.2
sulfonamides							
sulfamethoxazole	3.4 ± 0.4	2.3 ± 0.4	2.8 ± 0.5	1.98 ± 0.01	n.d.	n.d.	n.d.
sulfadimethoxine	9.4 ± 0.9	3.1 ± 0.5	3.0 ± 0.7	2.1 ± 0.1	n.d.	n.d.	n.d.
sulfadiazine	4.8 ± 0.6	7 ± 1	11.3 ± 0.5	5.97 ± 0.04	6.5 ± 0.8	n.d.	n.d.

[a] Units for all rate constants: in $10^{-5}\,s^{-1}$. Average values and standard deviations from two independent experiments are given. [b] Measured for buffered aqueous solutions (10 mM phosphate, pH 8.0) in the absence of DOM. [c] Measured for buffered aqueous solutions (10 mM phosphate, pH 8.0) in the presence of 2.5 mg_C L^{-1} Suwannee River fulvic acid and corrected for the light screening effect (Text S4, eq. S10). [d] Corrected rate constants (Text S4, eq. (S11)). [e] Correction had no effect on the significant digits. [f] n.d.: Not determined for the reasons explained in Text S4. [g] Evaluated in the time range 0 – 2160 s. [h] Conservative estimate calculated by subtracting $k^{obs}_{dir\_0.1}$. from $k^{obs,sc}_{SRFA\_5.0}$.

Table S5. $k_{DOM\_0.1}^{obs,c}$ **for DMOP in aqueous solutions of DOM isolates at various concentrations (pH 8.0)**

DOM Type	[DOM] / mg_C L^{-1}			
	1	2.5	5	10
SRFA	$(5.4 \pm 0.4) \times 10^{-3}$	$(1.7 \pm 0.1) \times 10^{-2}$	$(2.31 \pm 0.01) \times 10^{-2}$	$(4.3 \pm 0.5) \times 10^{-2}$
SRHA	$(8.11 \pm 0.02) \times 10^{-3}$	$(1.46 \pm 0.08) \times 10^{-3}$	$(3.1 \pm 0.1) \times 10^{-2}$	$(4.4 \pm 0.1) \times 10^{-2}$
PLFA	$(8 \pm 4) \times 10^{-4}$	$(2.5 \pm 0.2) \times 10^{-3}$	$(5.0 \pm 0.3) \times 10^{-3}$	$(1.16 \pm 0.03) \times 10^{-3}$

Table S6. $k_{DOM\_5.0}^{obs,c}$ **for DMOP in aqueous solutions of DOM isolates at various concentrations (pH 8.0)**

DOM Type	[DOM] / mg_C L^{-1}			
	1	2.5	5	10
SRFA	$(5.4 \pm 0.3) \times 10^{-4}$	$(1.49 \pm 0.09) \times 10^{-3}$	$(3.1 \pm 0.4) \times 10^{-3}$	$(6.1 \pm 0.4) \times 10^{-3}$
SRHA	$(8.6 \pm 0.2) \times 10^{-4}$	$(1.6 \pm 0.2) \times 10^{-3}$	$(3.52 \pm 0.05) \times 10^{-3}$	$(6.4 \pm 0.3) \times 10^{-3}$
PLFA	$(3.2 \pm 0.5) \times 10^{-4}$	$(1.3 \pm 0.1) \times 10^{-3}$	$(2.8 \pm 0.2) \times 10^{-3}$	$(5.1 \pm 0.5) \times 10^{-3}$

Text S5. Stability of 2-acetonaphthone and 4-cyanophenol during irradiation experiments of chemical model system solutions

The concentrations of the photosensitizer 2-acetonaphthone and of the electron-poor phenol 4-cyanophenol were also monitored during the irradiation experiments performed to study the transformation kinetics of 3,4-dimethoxyphenol (DMOP) in the chemical model system solutions. Figure S1 illustrates the typical evolution of concentration of DMOP, 2-acetonaphthone and 4-cyanophenol as a function of irradiation time for the highest (5.0 μM, Fig. S1a) and lowest (0.1 μM, Fig. S1b) initial concentrations of DMOP. In these two specific cases, after the whole irradiation period, the concentration of 2-acetonaphthone decreased by 7% and 1%, respectively, and the concentration of 4-cyanophenol decreased by 2% and 3%, respectively, compared to their initial concentration. These minor reductions, which are mostly even smaller than the analytical precision in the quantification of concentrations ($\approx$ 5%), confirm the stability of 2-acetonaphthone and 4-cyanophenol under the employed experimental conditions. Therefore, no corrections were applied to the determination of the pseudo-first-order rate constants k^{obs} for the transformation of DMOP.
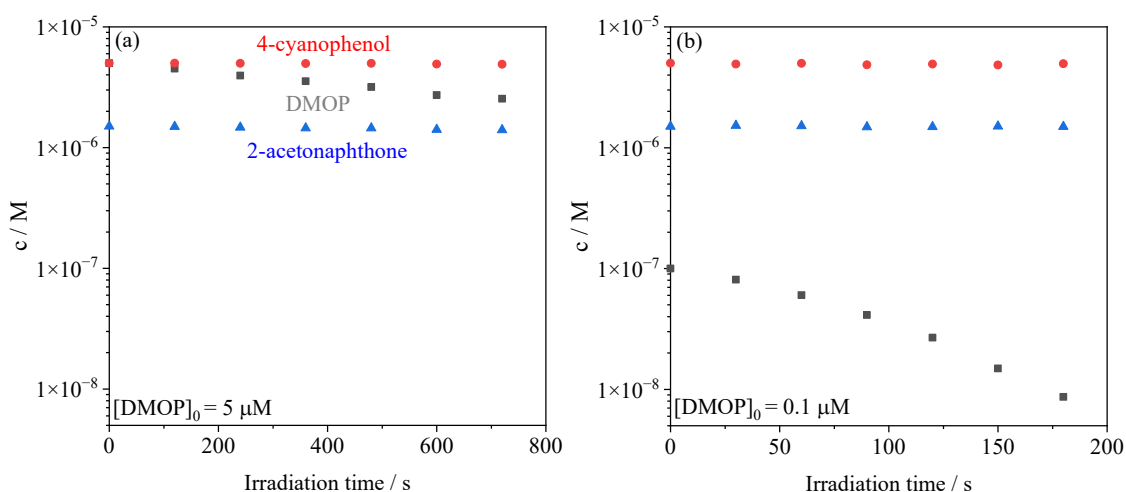

Fig. S1. Experimental runs of the concentrations of 3,4-dimethoxyphenol (DMOP, gray squares), 2-acetonaphthone (blue triangles), and 4-cyanophenol (red circles) for the irradiation of solutions (pH 8.0) with initial DMOP concentration of (a) 5 μM, and (b) 0.1 μM. Note the logarithmic scale of the y-axes. The initial concentrations of 2-acetonaphthone and 4-cyanophenol were 1.5 μM and 5.0 μM, respectively.

Text S6. Kinetic modelling for the system including 2-acetonaphthone as a photosensitizer, 4-cyanophenol as an electron-poor phenol, and 3,4-dimethoxyphenol (DMOP) as a target compound

The reactions considered for the modelling and explained in detail in the main paper, Section 3.4., are compiled in Table S8, together with details about the used rate constants.

Particular attention had to be paid to the determination of the first-order rate constant for the excitation of the photosensitizer 2-acetonaphthone (2-AN) to yield its excited triplet state ^{3}2-AN* (eq. (3) in the main paper), $k^f_{^32\text{-AN*}}$ (the superscript "f" stays for "formation"), which depends on the experimental conditions used for irradiation. To obtain this rate constant, the experimental value of the pseudo-first-order phototransformation rate constant of DMOP at an initial concentration of 5.0×10^{-6} M, $k^{obs}_{2\text{-AN,DMOP\_5.0}}$, was used. Since at this initial DMOP concentration the transformation of DMOP is almost exclusively induced by ^{3}2-AN*, for which the lifetime is not significantly affected by the presence of DMOP, the following equation holds:

$$k^{obs}_{2\text{-AN,DMOP\_5.0}} = k^r_{^32\text{-AN*,DMOP}} \times \left[\, ^32\text{-AN*}\right]_{ss} \tag{S12}$$

where $k^r_{^32\text{-AN*,DMOP}}$ is the second-order rate constant for the reaction of ^{3}2-AN* with DMOP leading to the transformation of the latter (the superscript "r" stands for "reaction" of DMOP), and [^{3}2-AN*]$_{ss}$ is the steady–state concentration of ^{3}2-AN*. This can be expressed as the ratio between the formation rate of ^{3}2-AN* (= $k^f_{^32\text{-AN*}} \times$ [2-AN]) and the pseudo-first-order deactivation rate constant of ^{3}2-AN*, $k^{d,air}_{^32\text{-AN*}}$:

$$\left[\, ^32\text{-AN*}\right]_{ss} = k^f_{^32\text{-AN*}} \times [2\text{-AN}] / k^{d,air}_{^32\text{-AN*}} \tag{S13}$$

Substituting eq. (S13) into eq. (S12) and solving for $k^f_{^32\text{-AN*}}$ yields:

$$k^f_{^32\text{-AN*}} = \frac{k^{obs}_{2\text{-AN,DMOP\_5.0}} \times k^{d,air}_{^32\text{-AN*}}}{k^r_{^32\text{-AN*,DMOP}} \times [2\text{-AN}]} \tag{S14}$$

To calculate $k^f_{^32\text{-AN*}}$ using eq. (S14), the values of the following three rate constants are needed:

1) $k^{obs}_{2\text{-AN,DMOP\_5.0}}$: This pseudo-first-order rate constant was determined in this study as 9.7×10^{-4} s^{-1}.

2) $k_{^{3}2\text{-AN*}}^{\text{d,air}}$: The first-order deactivation rate constant of $^{3}2\text{-AN*}$ in aerated aqueous solution (see eq. (4) in the main paper) was determined as 6.44×10^{5} s^{-1} in a previous study using laser flash photolysis (Canonica et al. 2000).

3) $k_{^{3}2\text{-AN*,DMOP}}^{\text{r}}$: This rate constant (corresponding to the reaction of eq. (5) in the main paper) was set equal to the second-order rate constant for the quenching of $^{3}2\text{-AN*}$ by DMOP (3.1×10^{9} M^{-1} s^{-1}) determined in a previous study by laser flash photolysis (Canonica et al. 2000). The validity of this approximation is supported by the high radical yields (approaching 1.0) determined for the quenching of the excited triplet states of aromatic ketones by phenoxides in water-acetonitrile solutions (Das and Bhattacharyya 1981).

Inserting the above-mentioned rate constant values and [2-AN] = 1.5×10^{-6} M into eq. (S14), one obtains $k_{^{3}\text{Sens*}}^{\text{f}}$ = 0.134 s^{-1}.

The second-order rate constant for the reaction of $^{3}2\text{-AN*}$ with the 4-cyanophenoxide ion (4-CN-PhO^{-}) leading to the formation of the 4-cyanophenoxyl radical (4-CN-PhO$^{\bullet}$, eq. (6) in the main paper) was estimated as $k_{^{3}2\text{-AN*,4-CN-PhO}^{-}}^{\text{r}}$ = 1×10^{9} M^{-1} s^{-1} based on the quenching rate constant determined for aqueous solutions of 4-cyanophenol at pH 6.0 (Canonica et al. 2000) and the high radical yields (approaching 1.0) determined for the quenching of the excited triplet states of aromatic ketones by phenoxides in water-acetonitrile solutions (Das and Bhattacharyya 1981). Note that the reaction of $^{3}2\text{-AN*}$ with undissociated 4-cyanophenol was neglected in the kinetic model because it is $\leq 10^{7}$ M^{-1} s^{-1} (Canonica et al. 2000).

The second-order rate constants for the reactions of 4-CN-PhO$^{\bullet}$ with DMOP (eq. (7) in the main paper) and its oxidation products DMOPox (eq. (8) in the main paper) are unknown. They were estimated as 2×10^{9} M^{-1} s^{-1}, i.e. the maximum values measured for the reactions of various phenoxyl radicals with different phenoxides (Steenken and Neta 1979).

Table S7. Overview of reactions and rate constants in the kinetic model

Reaction	Equation number (main paper)	Rate constant	Notes and references
2-AN $\xrightarrow{h\nu}$ ^{3}2-AN*	(3)	$k^{\mathrm{f}}_{^{3}2\text{-AN*}} = 0.134\ \mathrm{s^{-1}}$	determined in this study [a]
^{3}2-AN* $\rightarrow$ 2-AN	(4)	$k^{\mathrm{d,air}}_{^{3}2\text{-AN*}} = 6.44 \times 10^{5}\ \mathrm{s^{-1}}$	(Canonica et al. 2000)
^{3}2-AN* + DMOP $\rightarrow$ 2-AN + DMOP$_{\mathrm{ox}}$	(5)	$k^{\mathrm{r}}_{^{3}2\text{-AN*,DMOP}} = 3.1 \times 10^{9}\ \mathrm{M^{-1}\ s^{-1}}$	(Canonica et al. 2000) [a]
^{3}2-AN* + 4-CN-PhO^{-} $\rightarrow$ 2-AN + 4-CN-PhO$^{\bullet}$	(6)	$k^{\mathrm{r}}_{^{3}2\text{-AN*,4-CN-PhO}^{-}} = 1 \times 10^{9}\ \mathrm{M^{-1}\ s^{-1}}$	estimated based on (Canonica et al. 2000) [a]
4-CN-PhO$^{\bullet}$ + DMOP $\rightarrow$ 4-CN-PhO^{-} + DMOP$_{\mathrm{ox}}$	(7)	$k^{\mathrm{r}}_{4\text{-CN-PhO}^{\bullet},\mathrm{DMOP}} = 2 \times 10^{9}\ \mathrm{M^{-1}\ s^{-1}}$	Estimated based on (Steenken and Neta 1979) [a]
4-CN-PhO$^{\bullet}$ + DMOP$_{\mathrm{ox}}$ $\rightarrow$ 4-CN-PhO^{-} + DMOP$_{\mathrm{ox}}$	(8)	$k^{\mathrm{r}}_{4\text{-CN-PhO}^{\bullet},\mathrm{DMOP}_{\mathrm{ox}}} = 2 \times 10^{9}\ \mathrm{M^{-1}\ s^{-1}}$	Estimated based on (Steenken and Neta 1979) [a]

[a] For further explanations, see Text S6.

References

Canonica, S., Hellrung, B. and Wirz, J. (2000) Oxidation of phenols by triplet aromatic ketones in aqueous solution. The Journal of Physical Chemistry A 104(6), 1226-1232.

Canonica, S. and Hoigné, J. (1995) Enhanced oxidation of methoxy phenols at micromolar concentration photosensitized by dissolved natural organic material. Chemosphere 30(12), 2365-2374.

Das, P. and Bhattacharyya, S. (1981) Laser flash photolysis study of electron transfer reactions of phenolate ions with aromatic carbonyl triplets. The Journal of Physical Chemistry 85(10), 1391-1395.

Leresche, F., von Gunten, U. and Canonica, S. (2016) Probing the photosensitizing and inhibitory effects of dissolved organic matter by using *N,N*-dimethyl-4-cyanoaniline (DMABN). Environmental Science & Technology 50(20), 10997-11007.

Morowitz, H.J. (1950) Absorption effects in volume irradiation of microorganisms. Science 111(2879), 229-230.

Neta, P. and Grodkowski, J. (2005) Rate constants for reactions of phenoxyl radicals in solution. Journal of Physical and Chemical Reference Data 34(1), 109-199.

Neta, P., Huie, R.E. and Ross, A.B. (1990) Rate constants for reactions of peroxyl radicals in fluid solutions. Journal of Physical and Chemical Reference Data 19(2), 413-513.

Rosario-Ortiz, F.L. and Canonica, S. (2016) Probe compounds to assess the photochemical activity of dissolved organic matter. Environmental Science & Technology 50(23), 12532-12547.

Schmitt, M., Erickson, P.R. and McNeill, K. (2017) Triplet-state dissolved organic matter quantum yields and lifetimes from direct observation of aromatic amine oxidation. Environmental Science & Technology 51(22), 13151-13160.

Sharpless, C.M. (2012) Lifetimes of triplet dissolved natural organic matter (DOM) and the effect of $NaBH_4$ reduction on singlet oxygen quantum yields: Implications for DOM photophysics. Environmental Science & Technology 46(8), 4466-4473.

Steenken, S. and Neta, P. (1979) Electron-transfer rates and equilibria between substituted phenoxide ions and phenoxyl radicals. Journal of Physical Chemistry 83(9), 1134-1137.

Wenk, J., von Gunten, U. and Canonica, S. (2011) Effect of dissolved organic matter on the transformation of contaminants induced by excited triplet states and the hydroxyl radical. Environmental Science & Technology 45(4), 1334-1340.

Zepp, R.G., Schlotzhauer, P.F. and Sink, R.M. (1985) Photosensitized transformations involving electronic energy transfer in natural waters - Role of humic substances. Environmental Science & Technology 19(1), 74-81.